Sol–Gel Assisted Inkjet Hologram Patterning

*Aleksandr V. Yakovlev, Valentin. A. Milichko, Vladimir. V. Vinogradov, and Alexandr V. Vinogradov**

Hereby, it is presented for the first time a method of producing holographic text and images using inkjet printing. For this purpose, colorless TiO_2 ink with a high refractive index is used and deposited on top of exposed poly(ethylene terephthalate)-based microembossed paper by an inkjet printer. Nanoscale coating the paper containing printed text or graphics with transparent polymers or lacquers provides an optical effect of selective preservation of the holographic pattern. The resulting image is preserved only at the site of the colorless ink with a high refractive index from an inkjet printer, allowing to quickly generate any image with a holographic effect. Achieving these results has succeeded through the use of a colloidal dispersion of nanocrystalline titania with a refractive index of 1.75 ± 0.08 in the entire visible range, which meets inkjet rheological requirements. It is shown that the diffraction effect and optical transparency in the visible region are fully preserved. For the first time, it is demonstrated the importance of chemically prepared nanomaterials and nanostructures for an application in the field of holography.

1. Introduction

Computer generated holography is a widely used technology in diverse applications, ranging from authentication and optical data storage to interferometry, particle trapping, and phase conjugation.[1–5] Holograms typically utilize dielectric structures realized by laser writing,[6] direct machining, or e-beam lithography.[7] The ultimate challenge for manipulating a light beam and producing a holographic effect is therefore the control of the vector field with a single optical element, that is, of the spatial distribution of amplitude, phase, and state of polarization. Holograms produced using these criteria, which were called rainbow holography,[8] are the most popular today and their production is increasing annually. Given the complexity of manufacturing such holography, scalability is achieved by employing template printing using special inks that dry by oxidation and/or ultraviolet curing.[9,10] Thus, one may obtain either a holographic paper, i.e., paper having a 3D variable structure, or a single image with a holographic effect in the form of text or pictures. The process of transferring the template pattern onto the polymer tape can take from several hours to several days depending on the complexity of the workpiece design. Methods for affordable and fast printing of individual images with a holographic effect, which would promote a rapid development of this area of knowledge and technology, have not been found yet. In this regard, our research is obviously novel, allowing production of a hologram of any shape in no more than a few minutes by an inkjet printer using TiO_2 ink. For this purpose, one needs to camouflage a holographic film by ink with high refractive index (HRI) (**Figure 1**).

As mentioned previously, the holographic and/or diffraction paper is known as an optically variable device, i.e., the image appearance varies depending on the light source, light angle, and the viewing angle. The imagery itself is reproduced on the surface of the paper, or other substrate, from an original holographic master by microembossing into a coating on the surface of the paper. The refractive index (RI) of such paper, which is usually produced from a UV-curable polymer, is in the range of 1.3–1.59.[11] Saving the microrelief from involving materials with the same RI, for example, moisture and fats from the air, is carried out in several ways. For instance, the surface is then vacuum metalized to provide a very bright, shiny, metallic finish that brings out the holographic imagery and makes it visible.[12] To produce transparent holograms, the microstructure is coated with a transparent dielectric layer with HRI using vacuum deposition or polymers with RI no less than 1.7.[13] We used this peculiarity of preserving the diffraction effect of rainbow holography to produce holograms with a predetermined shape. For this purpose, special ink based on an aqueous colloidal solution of nanocrystalline titania was prepared. Applying the ink to the surface of exposed embossed holographic paper provides a nanometer highly refractive layer, which prevents the disappearance of the diffraction effect by applying a lacquer or polymer layer with low RI at the third stage (Figure 1). Visualization of the mechanism of this process is shown in Figure 1.

Local preservation of the holographic pattern is provided by several parameters implemented in this study: 1) the refraction index of embossed holography and polymer-coating is identical; 2) an average refractive index of 1.75 for inkjet titania within the visible range; 3) inkjet titania film and final lacquer layer do not change light transmission of holographic paper, thus fully retaining the diffraction effect; and 4) high adhesion of layers

A. V. Yakovlev, Dr. V. A. Milichko,
Dr. V. V. Vinogradov, Dr. A. V. Vinogradov
ITMO University
Kronverksky Pr. 49, St. Petersburg 197101
Russia
E-mail: vinogradoffs@mail.ru

DOI: 10.1002/adfm.201503483

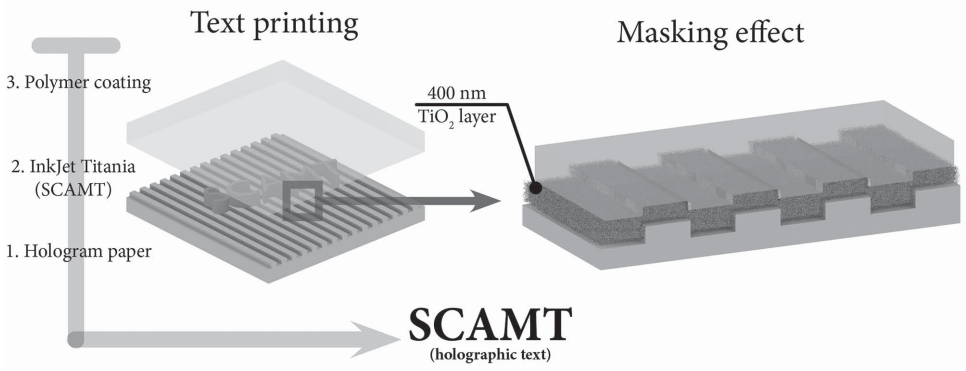

Figure 1. An inkjet titania layer on embossed holographic paper for direct data visualization.

2 and 3 to the substrate (Figure 7). As shown in this work, any images and text may be produced under the above conditions. Moreover, given the high porosity of the nanoparticle layer of TiO_2[14,15] and its hydrophilic properties,[16] one may deposit conventional dye-based inks on top of an HRI layer, thus combining multiple optical effects in thin layers.

2. Results and Discussion

To maintain high contrast and enhance the optical effect of holographic paper, it is extremely important to apply a protective transparent dielectric layer with a high RI.[8] Colloidal titania-based inks completely meet these requirements[16] and after drying form an optically transparent coating with HRI. Key features of these nanoproducts are a high degree of crystallinity and the ability of a sol–gel phase transition in the drying process. Among the known techniques for producing titania using solution methods without an annealing stage, achieving a refractive index of 1.75 ± 0.08 in the visible region was previously impossible. In this connection, one often uses the calcined powder of nanocrystalline TiO_2 dispersed in a polymer.[16–18] However, this approach is not suitable for inkjet and does not provide an application of thin layers with a uniform distribution of refractive phase. In our study, we used low-temperature sol–gel synthesis of nanocrystalline TiO_2[14] with RI = 1.75 at 400 nm. To avoid the photocatalytic effect of TiO_2 on the organic phase, its layer was coated with a lacquer, Figure 1 right side, which prevents a contact between the photocatalyst and the H_2O molecules and makes it inactive and safe for a long operation. In this study, we used a nanocrystalline TiO_2 sol obtained using only nitric acid as a protonating agent without any stabilizers. To reduce the surface tension and increase the rate of ink drying, we modified its production process, adapting inkjet printing to uniform application. Moreover, the absence of organic stabilizers, such as polymers and surfactants, promotes the rapid condensation of sols during evaporation of the solvent, ensuring high adhesion to the microembossed paper by providing the sol–gel transition directly on the substrate. The result is a coating that provides high adhesion to the substrate as opposed to using conventional vacuum deposition (**Figure 2**).

It is clearly seen that adhesion of the TiO_2 coating deposited by a vacuum technique on embossed holographic paper is very poor, Figure 2a,b in contrast to inkjet printable titania, Figure 2c,d. This is due to the fact that the vacuum technique requires a preliminary activation of the holographic paper film surface in an oxygen plasma flow to form active hydroxyl groups on the polymer surface,[19,20] unlike sol–gel coatings which provide a physical cross-linking to the surface in the drying process (Figure 2 and **Figure 3**).[21,22] These conclusions are confirmed by the cross-section data obtained after applying TiO_2 using every method (Figure 3). To assess the adhesion properties, the coatings were exposed to a classical adhesive tape peel test. Figure 3 shows SEM images of coatings after five tests.

The resulting images demonstrate high adhesion properties of TiO_2 when applied using an inkjet printer (Figure 3c,d). This conclusion is confirmed by an EDS profilogram (red line) (Figure 3a,c). It is clearly seen that the vacuum-deposited active TiO_2 layer is easily separated from the substrate (Figure 3a), as indicated by the broken EDS line. After five adhesive tape tests, the continuity of the coating is maintained at a level of no more than 50%. Figure 2b shows that the TiO_2 coating is not fixed to the polymer substrate after vacuum deposition, which facilitates its easy separation, deteriorating resistance to mechanical stress. On the other hand, colloidal ink is more resistant

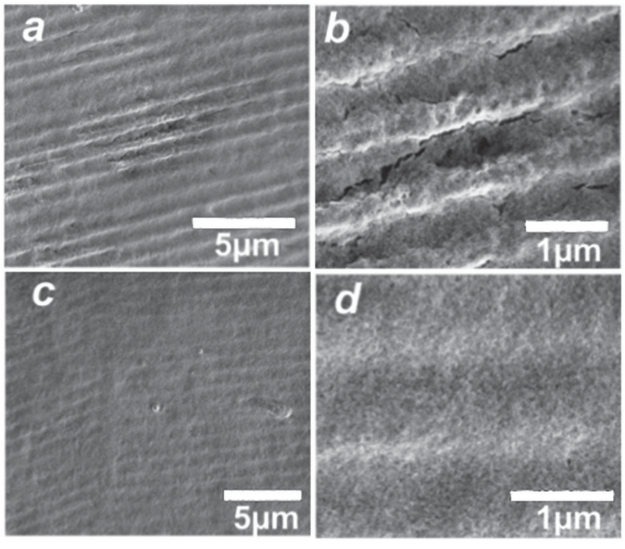

Figure 2. SEM images of titania film on holographic paper deposit by a,b) a vacuum technique and c,d) inkjet printing.

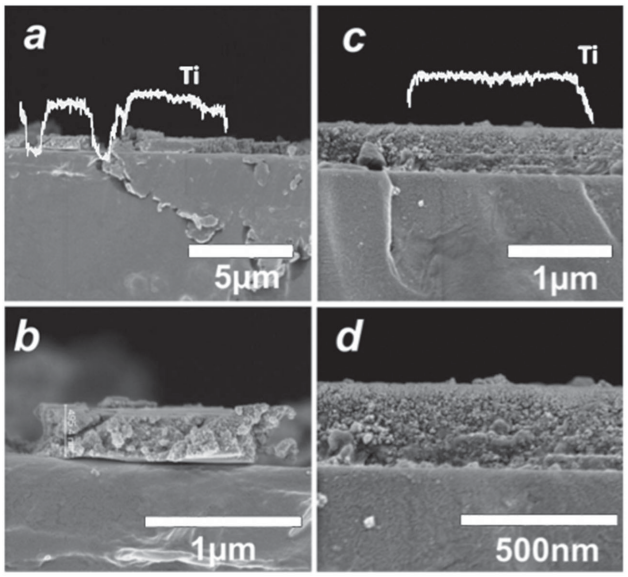

Figure 3. Cross-section SEM images and EDS (white lines) of a titania film on holographic paper deposit by a,b) a vacuum technique and c,d) inkjet printing after five adhesive tape tests.

to external mechanical impact and provides high adhesion to holographic paper.

EDS image mapping for inkjet sol–gel titania, Figure 3c, illustrates the continuity and complete preservation of the coating after five adhesive tape peel tests, Figure 3d, as well as a close contact between the deposited TiO_2 layer and the polymer substrate without preliminary hydroxylation of the substrate surface.

Optical properties of nanocrystalline titania inkjet coatings, such as reflectance spectrum and refractive index dispersion, are shown in **Figure 4**. Since the coating is positioned between the two isotropic media (air and 2 mm fused silica substrate), at certain radiation wavelengths one may observe reflection minima in the spectra (i.e., the radiation does not "see" the film, but is in fact reflected from the "virtual" boundary between substrate and air). This reflection coefficient for the air–glass boundary is shown as a red dashed line in Figure 4.[23]

The reflection coefficient maxima in Figure 4 correspond to the positive interference of a specific wavelength radiation reflected from the air–inkjet, inkjet–fused silica boundaries.

In this case, regardless of the film thickness, the reflection coefficients at these wavelengths are determined by the expression[24] $R = \left(\frac{n_1 n_3 - n_2^2}{n_1 n_3 + n_2^2}\right)^2$, where n_2 is the refractive index of the film at the same wavelengths, and n_1 and n_3 are the refractive indices for air and fused silica, respectively. Thus, from experimental data on reflection coefficients, Figure 4, one can derive refractive index dispersion of the films. This relationship is shown in Figure 4, and the scatter of the experimental values for refractive indices obtained from a large series of experiments (see the Experimental Section), allowed us to estimate a refractive index of 1.75 ± 0.08 in the entire visible range.

The high refractive index of inkjet TiO_2 ink (RI ≈ 1.75), in contrast to that for the polymer holographic paper (RI ≈ 1.41), leads to camouflaging the microembossed surface upon coating with a lacquer and can preserve the light diffraction at the treated site. Moreover, the optical density of the formed inkjet TiO_2 coatings was found to be on a par with that for calcined materials.[25] We used these properties to produce holographic images, **Figure 5**, by selectively applying HRI ink with an inkjet printer and subsequently depositing a lacquer layer with a low RI (1.34) by a Meyer bar like holographic paper. Multilayer packaging of the formed structure is shown in Figure 1. Figure 5 shows photographs of inkjet printing of holographic text, Figure 5a, and images, Figure 5b, obtained by the new method.

The disappearance of the holographic effect in the area not treated by TiO_2 ink is due to the fact that the refraction index of rainbow holography paper (1.41) and lacquer layer (1.34) are identical, which causes the light not to be refracted and to reflect at the interface between phases 1 and 3, Figure 1, passing through the microembossed structure unchanged. On the other hand, the presence of a thin, transparent layer of TiO_2 results in camouflaging the effect of microembossed structure. This peculiarity not only causes refraction at the paper–lacquer interface but also increases the intensity of the reflected beam, increasing the main holographic effect. Clarity of the resulting pattern is determined exclusively by specifications of an inkjet printer and

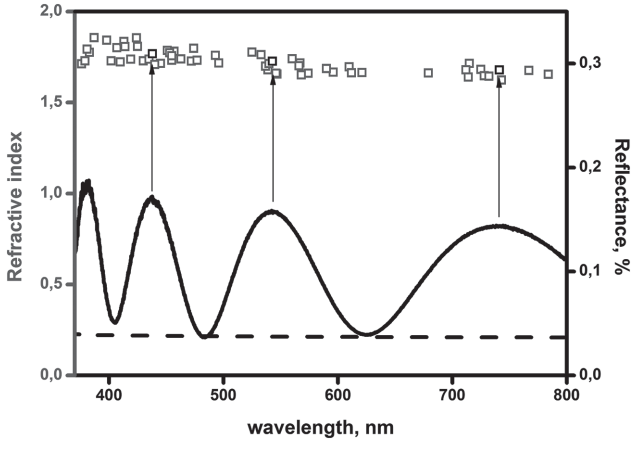

Figure 4. Dispersion of the refractive index for TiO_2 inkjet film (squares) and reflection spectrum of a 500 nm thick TiO_2 inkjet film on a 2 mm fused silica substrate in the air (solid line); reflection from fused silica substrate (dotted line).

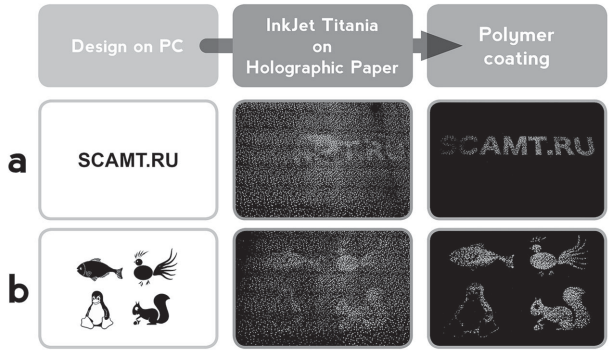

Figure 5. Photographs of a) text and b) images of inkjet hologram prepared using titania sol as an HRI thin film.

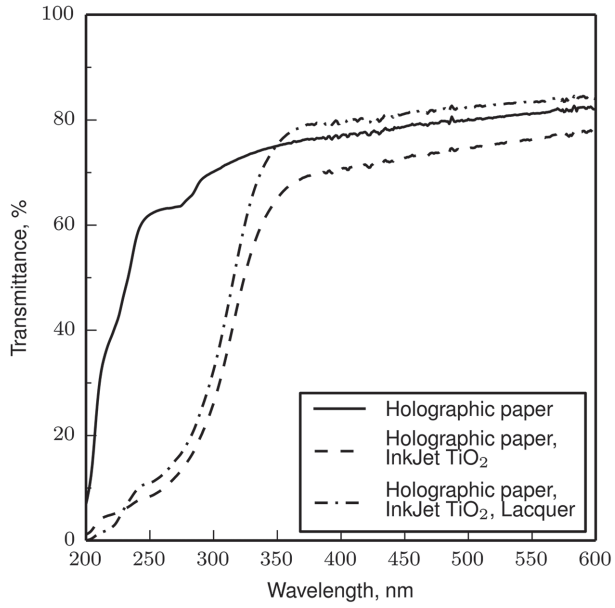

Figure 6. Transmission spectra of holographic paper (blue line) after applying inkjet titania (red line) and after coating a lacquer by a Meyer bar.

its resolution. Figure 5 clearly shows that the diffraction effect of holographic paper has not lost its brightness and clearly conveys the essence of the text and pictures. The presence of an HRI inkjet thin layer on top of holographic paper increases the reflection coefficient on average by two orders of magnitude compared to that for the paper coated only with polymers.

According to the transmission spectra, **Figure 6**, the transparency of the final heterostructure in the visible region remains virtually unchanged. Even a 2% increase in light transmission of the resulting heterostructure is observed.

High mechanical hardness of TiO_2 coatings and their adhesion to PET holographic paper are confirmed by the results of tests to determine the coefficient of friction. For this, the shear strength between the layers was investigated versus time, as shown in **Figure 7**.

It was found that the strength of the interaction between the TiO_2 film and holographic paper, 0.557^{min}, is similar to the interaction of a lacquer with pure PET, 0.637. This demonstrates the high affinity of the films and their high stability like usual organic substrate. The inversely proportional dependence of the static friction coefficient on thickness of the applied TiO_2 layer, Figure 8 inset, allowed us to determine the most suitable parameters of mechanical hardness for a TiO_2 inkjet film. The measurement range for friction coefficients depending on the thickness of a deposited TiO_2 layer corresponded to contact interaction of classic organic polymers. In this regard, high adhesion of layers to each other is provided. The determined values are in line with the data on the optical transparency, achieving the camouflaging effect, and rheological properties as the most optimal composition for hologram inkjet printing.

3. Conclusions

We have demonstrated here an effective and economic strategy for the development of inkjet printing of holograms using holographic paper. This technique was made possible by employing an inkjet printer to apply a nanocrystalline TiO_2 layer with HRI, which upon coating the final lacquer layer provides a protective function for the microrelief, preserving the diffraction effect in the treated area. The formed structure does not change the optical transmittance and thus retains the image contrast. Moreover, compared to the conventional vacuum technique the sol–gel TiO_2 jet has a high adhesion and forms a dense heterostructure with increased mechanical hardness. We believe that the new method will dramatically expand possibilities in visualizing images using holograms and significantly simplify the process of their manufacturing.

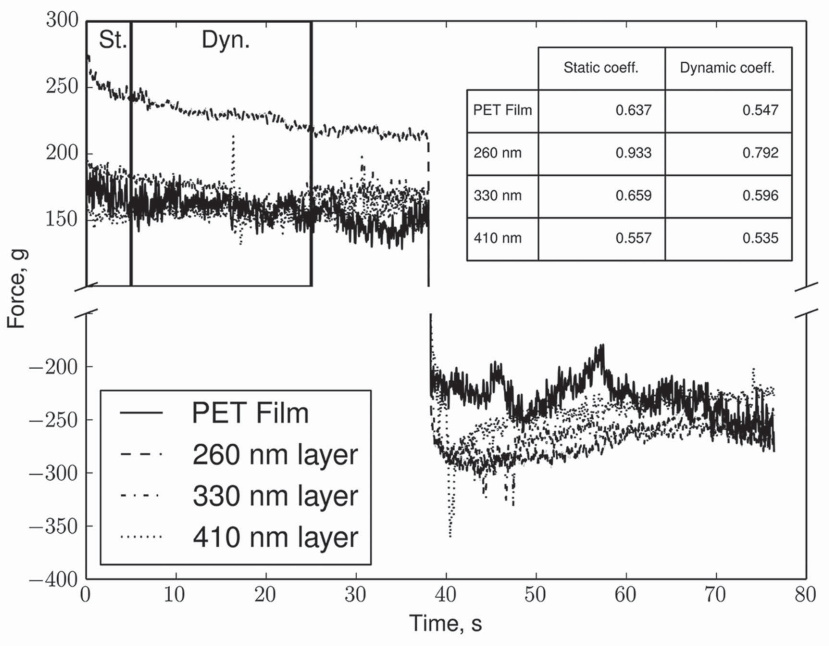

	Static coeff.	Dynamic coeff.
PET Film	0.637	0.547
260 nm	0.933	0.792
330 nm	0.659	0.596
410 nm	0.557	0.535

Figure 7. Shear strength between TiO_2 and holographic paper versus time and interrelationship of the TiO_2 layer thickness and the static coefficient of friction.

4. Experimental Section

4.1. Chemicals

Titanium(IV) isopropoxide (TIP) 97% (Aldrich), ethanol >96% (Aldrich), nitric acid (≈65%), isobutyl methacrylate 97% (Aldrich) as an lacquer dissolved in acetone 99,6% (Aldrich), and deionized water (<5 μS cm^{-1}) were used without additional purification.

4.2. Synthesis of TiO_2 Ink

TiO_2 nanoparticles were synthesized by hydrolysis of TIP in deionized water, under vigorous stirring (1000 rpm) and using nitric acid as a protonating agent. TIP was injected dropwise into the

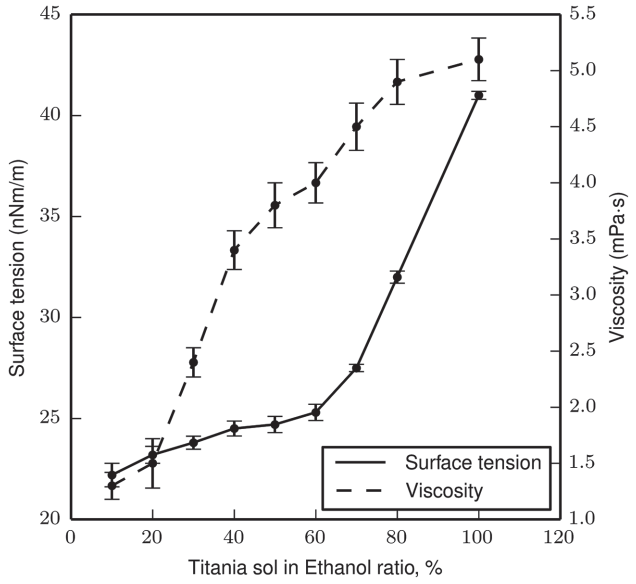

Figure 8. The dependence of the viscosity and surface tension of the tested formulations on the dilution.

deionized water for 3 min. Detailed synthesis scheme is described in ref.[14]. As shown previously,[14] a nanocrystalline titania sol in the anatase phase forms within 6 h. To change the surface tension and viscosity, the aqueous solution of the sol was mixed with ethanol to a certain TiO_2(sol)–ethanol volume ratio (**Figure 8**, **Table 1**). The resulting solution was homogenized for 12 d to complete the solvation. The sol solution was then decanted in a rotary evaporator under reduced pressure at 50 °C. Table 1 and Figure 8 summarize the dilution ratios and corresponding densities of the printing formulations. Figure 1 depicts the viscosity and surface tension of the tested formulations. Formulation, containing 30 vol% of the stock TiO_2 sol, was identified as optimal for providing a balanced compromise between printings. The drop dynamics and film formation can be predicted to a certain degree by theoretical descriptors such as Z number ($Z = \sqrt{(d \cdot \sigma \cdot \delta)}/\eta$, where δ is the density, d is the diameter of the nozzle, σ is the surface tension, and η is the viscosity of the reliability and sufficient dry mass content. Table 1 also gives the values of the Z number that were used as the indicator of drop formation and printability (e.g., capillary break-off length and time, droplet volume, and satellite formation). While some theories predict a stable drop formation in drop-on-demand systems when $Z > 2$,[26] others determined that a printable fluid should have a Z value between 1 and 10.[26] It is also known that the lower limit is governed by the viscosity of the fluid and its printing ability, while the upper limit is determined by the point at which multiple drops are formed instead of a single droplet.[26] In our study, the Z values were in the range of 4–9, which is in full agreement with current theories. Viscosity was determined by a Brookfield HA/HB viscometer, and surface tension by a Kyowa DY-700 tensiometer.

Table 1. Summarized properties of printing solutions.

$TiO_{2(sol)}$/ethanol [%]	Surface tension [mN m^{-1}]	Viscosity [mPa s]	Z number
10	22.2 ± 0.6	1.3 ± 0.2	9.47
20	23.2 ± 0.4	1.5 ± 0.2	8.88
30	23.8 ± 0.3	2.4 ± 0.1	5.72
40	24.5 ± 0.4	3.4 ± 0.1	4.14
50	24.7 ± 0.4	3.8 ± 0.2	3.77
60	25.3 ± 0.4	4.0 ± 0.2	3.67
70	27.5 ± 0.2	4.5 ± 0.2	3.43
80	32.0 ± 0.3	4.9 ± 0.2	3.41
100	41.0 ± 0.2	5.1 ± 0.2	3.72

4.3. Applying TiO_2 Ink on the Surface of Microembossed Holographic Paper

The TiO_2 ink was deposited on commercially available microembossed PET film with a thickness of 20 μm, Figure 1, and with a refractive index of 1.41 (λ = 400 nm). The film was not preliminarily treated and did not have any layers modifying its surface. To print titania ink, a desktop office printer Canon Pixma IP 2840 with a drop volume of 2 pL was used. For this purpose, a holographic film was fixed on a regular A4 sheet, providing a predetermined thickness of the paper. The ink was placed in the cartridge without additional modification. The thickness of an inkjet TiO_2 layer after drying in the air and removal of the solvents did not exceed 500 nm with an RI of no less than 1.75 ± 0.08 in the entire visible range.

4.4. Coating Microembossed Holographic TiO_2-Containing Paper with a Lacquer

A layer of acrylic lacquer, consisting of a 1:1 solution of isobutyl methacrylate in acetone, was deposited by a Meyer bar with a nickel wire with a 10 mm diameter and a 6 μm thickness of coating the wet layer. The thickness of the formed layer after drying did not exceed 4 μm, yielding a smooth glossy coating having a refractive index of 1.34 (λ = 400 nm). Time of complete drying of the lacquer layer and the formation of the finished image did not exceed 30 min.

4.5. Characterization Techniques

Wide-range X-ray powder diffraction data have been processed using Bruker D8 Advance equipment with CuKα (λ = 154.18 pm).

To study the TiO_2 inkjet film using scanning electron microscopy (SEM) including cross section and EDS analysis, after complete drying in a vacuum desiccator, was investigated without additional sputtering with an ultrahigh resolution electron microscope Magellan 400L (Field Emission Inc.). Optical reflection measurement at normal incidence was carried out to obtain refractive indices for TiO_2 ink layer within the range of 400–800 nm.

For this experiment the confocal optical scheme was arranged. The incident unpolarized light from a halogen lamp (HL-2000-FHSA) was focused on the film surface through a 50× microscope objective (Mitutoyo M Plan APO, NA 0.55). Reflected light was collected through the same objective and then analyzed by a spectrometer (HORIBA LabRam HR) with a cooled CCD camera (Andor DU 420A-OE) and a 150 g mm^{-1} diffraction grating. The obtained spectra were normalized by the known spectrum of the halogen lamp. The reflectance spectra from different points of the film with different thickness allowed us to estimate the error for refractive index at various wavelengths. Transmittance spectra of new inkjet hologram were measured using a Cary 8454 UV–vis Diode Array System. TA.XTPlus texture analyzer (Stable Micro Systems, UK) operated with Horizontal Friction System (A/HFS) was employed to determine the shear strength of TiO_2 films (test speed: 2.5 mm s^{-1} and distance: 95 mm).

Acknowledgements

This work was supported by the Russian Government, Ministry of Education (research was made possible due to financing provided to the Customer from the federal budget aimed at maximizing Customer's

competitive advantage among world's leading educational centers). The authors are grateful to the Center for Nanoscience and Nanotechnology at Hebrew University for assistance in performing HRTEM and SEM experiments. The authors are grateful to Dr. P. Dmitrikiv from Packvision and V. Rigin from Interfoil for help with holographic papers delivery.

Received: August 18, 2015
Revised: September 18, 2015
Published online: November 17, 2015

[1] L. Dhar, K. Curtis, T. Fäcke, *Nat. Photonics* **2008**, *2*, 403.
[2] Y. Yifat, M. Eitan, Z. Iluz, Y. Hanein, A. Boag, J. Scheuer, *Nano Lett.* **2014**, *14*, 2485.
[3] J. Liesener, M. Reicherter, T. Haist, H. J. Tiziani, *Opt. Commun.* **2000**, *185*, 77.
[4] G. W. Burr, I. Leyva, *Opt. Lett.* **2000**, *25*, 499.
[5] A. James J. Cowan, *U.S. patent US4839250*, **1988**.
[6] E. N. Leith, A. Kozma, J. Upatnieks, J. Marks, N. Massey, *Appl. Opt.* **1966**, *5*, 1303.
[7] T. Hessler, M. Rossi, R. E. Kunz, M. T. Gale, *Appl. Opt.* **1998**, *37*, 4069.
[8] S. A. Benton, *J. Opt. Soc. Am.* **1969**, *59*, 1545.
[9] H. Peng, D. P. Nair, B. A. Kowalski, W. Xi, T. Gong, C. Wang, M. Cole, N. B. Cramer, X. Xie, R. R. McLeod, C. N. Bowman, *Macromolecules* **2014**, *47*, 2306.
[10] P. K. Tapaswi, M.-C. Choi, K.-M. Jeong, S. Ando, C.-S. Ha, *Macromolecules* **2015**, *48*, 3462.
[11] M.-C. Choi, J. Wakita, C.-S. Ha, S. Ando, *Macromolecules* **2009**, *44*, 5112.
[12] A. K. Yetisen, I. Naydenova, F. da C. Vasconcellos, J. Blyth, C. R. Lowe, *Chem. Rev.* **2014**, *114*, 10654.
[13] a) T. Higashihara, M. Ueda, *Macromolecules* **2015**, *48*, 1915; b) W. Decker, S. Early, J. Muaricio, A. Bartholomay, *U.S. patent WO 2004003668 A1*, **2003**.
[14] A. V. Vinogradov, V. V. Vinogradov, *J. Am. Ceram. Soc.* **2014**, *97*, 290.
[15] A. V. Vinogradov, V. V. Vinogradov, *RSC Adv.* **2014**, *86*, 45903.
[16] L.-H. Lee, W.-C. Chen, *Chem. Mater.* **2001**, *13*, 1137.
[17] H. I. Elim, B. Cai, Y. Kurata, O. Sugihara, T. Kaino, T. Adschiri, A.-L. Chu, N. Kambe, *J. Phys. Chem. B* **2009**, *113*, 10143.
[18] J-G. Liu, Y. Nakamura, T. Ogura, Y. Shibasaki, S. Ando, M. Ueda, *Chem. Mater.* **2008**, *20*, 273.
[19] T. Cavallin, N. Habra N, M. Casarin, F. Bordin, A. Sartori, M. Favaro, R. Gerbasi, G. Rossetto, *J. Nanosci. Nanotechnol.* **2011**, *11*, 8079.
[20] E. J. Szili, S. Kumar, R. S. Smart, R. Lowe, E. Saiz, N. H. Voelcker, *Surf. Sci.* **2008**, *602*, 2402.
[21] M. Langlet, A. Kim, M. Audier, C. Guillard, J. M. Herrmann, *Thin Solid Films* **2003**, *429*, 13.
[22] M. Langlet, A. Kim, M. Audier, C. Guillard, J. M. Herrmann, *J. Mater. Sci.* **2003**, *38*, 3945.
[23] L. Gao, F. Lemarchand, M. Lequime, *J. Eur. Opt. Soc.* **2013**, *8*, 13010.
[24] a) J. Ward, J. Cooper, E. W. Smith, *J. Quant. Spectrosc. Radiat. Transfer* **1974**, *14*, 555; b) M. Born , E. Wolf, *Principles of optics: electromagnetic theory of propagation, interference and diffraction of light.*, Cambridge University Press, Cambridge, UK **1999**.
[25] N. Shahruz, H. M. Moghaddam, *J. Dispersion Sci. Technol.* **2014**, *35*, 1174.
[26] a) J. E. Fromm, *IBM J. Res. Dev.* **1984**, *28*, 322; b) N. Reis, B. Derby, in *Ink Jet Deposition of Ceramic Suspensions: Modelling and Experiments of Droplet Formation*, Cambridge University Press, Cambridge, UK, **2000**, p. 65; c) D. Jang, D. Kim, J. Moon, *Langmuir* **2009**, *25*, 2629.